Corrosion Science 127 (2017) 280–290

Contents lists available at ScienceDirect

Corrosion Science

journal homepage: www.elsevier.com/locate/corsci

Effect of extrusion on corrosion properties of Mg-2Ca-χAl (χ = 0, 2, 3, 5) alloys

Peng-peng Wu[a], Fang-jun Xu[a], Kun-kun Deng[a,*], Fu-yin Han[a], Zhong-zhong Zhang[a], Rui Gao[b]

[a] Shanxi Key Laboratory of Advanced Magnesium-based Materials, College of Materials Science and Engineering, Taiyuan University of Technology, Taiyuan 030024, PR China

[b] CNNC Xinneng Nuclear Engineering Co., Ltd, Taiyuan 030024, PR China

ARTICLE INFO

Keywords:
A. Mg-Al-Ca alloys
B. EIS
B. Polarization
B. Weight loss
C. Passive films

ABSTRACT

Effect of extrusion on the microstructures and corrosion properties of Mg-2Ca-χAl (χ = 0, 2, 3, 5 wt.%) alloys were investigated in present work. Results showed that the precipitated phase changed from Mg_2Ca and $(Mg, Al)_2Ca$ to Al_2Ca with the increase of Al content. Corrosion results indicated that the addition of Al could improve the corrosion resistance of Mg by the formation of protective $(Mg, Al)_2Ca$ and Al_2Ca. The as-cast alloys showed uniform corrosion mechanism while the as-extruded Mg-Al-Ca alloys presented local corrosion characteristic. Above different corrosion mechanisms were illustrated and analyzed.

1. Introduction

Magnesium (Mg) alloys have considerable potential applications in automotive industries and aerospace due to the low density, high specific stiffness and strength, as well as good environmental friendliness [1,2]. However, the poor corrosion performance creates one obstacle to its application as industrial material. It is known that the electrochemical potential of Mg alloy is very low [3,4]. Nevertheless, the porous $Mg(OH)_2$ film formed on the magnesium is not stable and cannot act as the passive film like Al_2O_3 on the surface of Al [5]. Above two reasons may be responsible for its poor corrosion resistance.

To improve the mechanical properties and corrosion resistance of Mg alloys, some practical and economical elements like Al [6,7] and Ca [8,9] were added. Bahman [7] studied the effect of Al on the microstructure and corrosion behavior of Mg-Al-Zn-Ca alloy. Result proved that the addition of Al up to 3 wt.% considerably improved the anticorrosive behavior due tograin refinement. Whereas, addition of Al more than 3 wt.% led to dramatically deteriorated corrosion resistance due to the acceleration of micro-galvanic couples which caused by the formation of net-like intermetallic compounds ($Mg_{17}Al_{12}$ phase) at grain boundaries. While the formation of $Mg_{17}Al_{12}$ phase can be suppressed by the addition of Ca [8,10]. Yang et al. studied the effect of Ca addition on the corrosion behavior of Mg-Al-Mn alloys [8], the the best corrosion resistance could be obtained when that content of Ca is 2 wt. %. This phenomenon was attributed to the massive and discontinuous $(Mg, Al)_2Ca$ phase, which acted as a sacrificial anode to protect the Mg matrix. It means that the corrosion resistance of Mg alloys can be improved by the addition of Ca. Category of secondary phase containing Ca had already been confirmed in Mg-Al-Ca alloys [10–12], which found that the Mg_2Ca, $(Mg, Al)_2Ca$ and Al_2Ca phase could be formed in sequence in the Mg-Al-Ca alloy with increasing Al contend. Whereas influence of these phase on corrosion behavior in Mg-Al-Ca alloys is still unclear.

To further improve the mechanical properties of Mg alloy, extrusion was also widely performed [10,13]. Based on our previous research [10], the secondary phase was broken into particles and the grains were refined effectively during the extrusion process of Mg-Al-Ca alloys. As a result, the mechanical properties of as-extruded Mg-Al-Ca alloys were improved obviously. However, the influnce of extrusion on the corrosion resistance of Mg-Al-Ca alloys containing different Al content is lacking in literature.

Thus, the Mg-2Ca alloys (wt.%) with 2 wt.%, 3 wt.% and 5 wt.% Al were fabricated in present work. By comparing the corrosion properties of as-cast and as-extruded Mg-Al-Ca alloy, the influence of extrusion on the corrosion properties of Mg-2Ca-χAl (χ = 0, 2, 3, 5 wt.%) alloys were investigated and analyzed.

2. Experimental procedure

2.1. Alloy preparation

The materials prepared in this study were the Mg-2Ca-χAl (χ = 0, 2, 3, 5, wt.%) alloys which were denoted as AC02, AC22, AC32, AC52, respectivley. Pure Mg (> 99.9%) ingot was melted with the protecting

* Corresponding author.
E-mail addresses: dengkunkun@tyut.edu.cn, jamsdk@163.com (K.-k. Deng).

http://dx.doi.org/10.1016/j.corsci.2017.08.014
Received 12 January 2017; Received in revised form 9 August 2017; Accepted 17 August 2017
Available online 31 August 2017
0010-938X/

Table 1
Chemical composition of the experimental alloys.

Materials	Chemical composition (wt.%)		
	Al	Ca	Mg
AC02	–	2.05	Bal.
AC22	2.26	2.17	Bal.
AC32	3.10	1.73	Bal.
AC52	5.03	1.67	Bal.

of anti-oxidizing gas atmosphere (1 vol.% SF_6 + 99 vol.% CO_2) in a steel crucible at 1033 K. Then the Al and Ca ingots (> 99.9%) were added into the melt. After 30 min stirring, alloy liquid was poured into a steel mold which was preheated at 623 K.

The as-cast ingots were machined into cylindrical samples with a dimension of Φ40 mm × 50 mm. After being kept at 623 K for 30 min, the samples were extruded at 623 K with the extrusion rate of 16:1 at a constant ram speed of 3 mm/s. During the extrusion process, the temperature was maintained to 623 K. Finally, the extruded bars cooled in room temperature with a diameter of 10 mm were attained.

2.2. Surface characterization

The chemical composition of the alloys is listed in Table 1. Microstructures of the as-cast and as-extruded alloys were observed by optical microscopy (OM) and scanning electron microscope (SEM) equipped with an energy dispersive X-ray spectroscopy (EDS). The morphology of as-extruded alloys was detected by the back scattered electron. All the samples were etched in acetic picral (2.1 g picric acid + 5 ml acetic acid + 5 ml distilled water + 35 ml alcohol). The average grain size and volume fraction of precipitates in the as-cast alloys were measured by Image-Pro Plus 5.0 software.

2.3. Corrosion measurements

2.3.1. Electrochemical measurements

The corrosion properties of as-cast and as-extruded alloys were measured by electrochemical experiments and weight loss measurement. The exposed area of samples was the transverse plane. All the samples used for the experiments were cut into cylinder (10 mm in diameter, 5 mm in thickness). After being grinded, the samples were ultrasonically cleaned in acetone for 15 min and dried by a drying apparatus.

For electrochemical tests, the samples were immersed into 3.5 wt.% NaCl solution at 25 ± 1 °C for 30 min to obtain a steady open circuit potential (OCP, V *vs*. SCE) before electrochemical impedance spectroscopy (EIS) test. A typical three-electrode cell with the specimen as the working electrode, a saturated calomel electrode (SCE) as the reference electrode, and a platinum plate with a dimension of 10 mm × 10 mm × 0.5 mm as the counter electrode was used. EIS tests were performed at open circuit potential over a frequency range from 10^5 to 10^{-2} Hz with an amplitude of 5 mV. To analysis the impedance data, the equivalent electrical circuit parameter was obtained by ZSimpWin software.

Potentiodynamic polarization tests were performed with a scan rate of 0.5 mV s^{-1} over a potential range from −1.9 V *vs*. SCE to −1.3 V *vs*. SCE. The samples were immersed into 3.5 wt.% NaCl solution at 25 ± 1 °C for 45 min before PDP tests. Due to the abnormal anodic behavior that Mg and its alloys typically show (negative difference effect [14,15]), the corrosion current density (i_{corr}, A cm^{-2}) was obtained by using the cathodic branch. Fig. 1 shows the schematic of method of obtaining corrosion current density. First, a horizontal line was drawn at the corrosion potential (E_{corr}, V *vs*. SCE). Then a slope was drawn at the potential range from E_{corr} to E_{corr} – 100 mV. After that, the abscissa of the point that the horizontal line and slope line intersect was considered as i_{corr}. Besides that, the breakdown potential (E_b, V *vs*. SCE) of passive film was also obtained from PDP curves, as Fig. 1 shows. All the electrochemical tests were performed for 3 times and the average values of OCP, E_{corr}, i_{corr} and E_b were obtained.

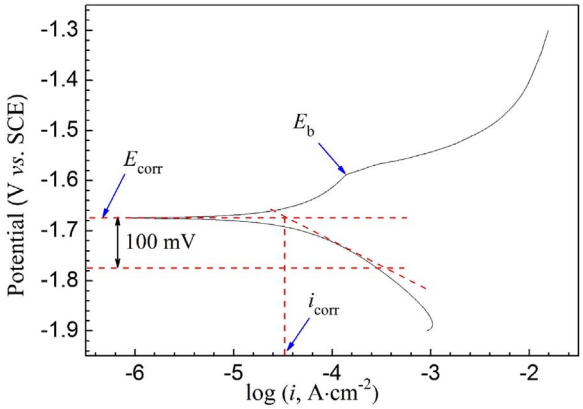

Fig. 1. The schematic of method of obtaining corrosion current density.

2.3.2. Weight loss measurement

Corrosion rates of the specimens were evaluated by weight loss measurement. The samples were immersed in 3.5 wt.% NaCl solution for 6 days at 25 ± 1 °C. Corrosion products formed on the samples were ultrasonically cleaned in chromic acid (200 g/L CrO_3 + 10 g/L $AgNO_3$ [16]) for 10 min at 80 ± 5 °C. Then the samples were cleaned by distilled water and dried in air. The dried specimens before and after immersion were weighted and the corrosion rates were calculated by the following equation [17]:

$$C_w = \frac{2.1\,\Delta m}{At} \quad (1)$$

where C_w is the corrosion rate in mm/year, Δm is the weight loss in mg, A is the surface area in cm^2, t is the total immersion time in day. The weight loss measurement was performed for 3 times and an average value of corrosion rate was calculated.

3. Results

3.1. Microstructure

Fig. 2(a)–(d) shows the optical micrographs of as-cast AC02, AC22, AC32 and AC52. With the Al addition, the dendrite cell size becomes significantly refined. The SEM micrographs of as-cast AC02, AC22, AC32 and AC52 are given in Fig. 3. Fig. 3(a) shows the presence of eutectic composed of Mg_2Ca and a-Mg in AC02. Eutectic phase formed as a result of the solidification of liquid, enriched with calcium solutes during the final stage of solidification. This phase is found either in grain interiors as isolated islands (indicated by dashed arrows) or along grain boundaries (indicated by line arrows). In AC22 alloy, the net-like distribution of Mg_2Ca phase is interrupted by the formation of lamellar $(Mg, Al)_2Ca$ phase (as shown in Fig. 3(b)). When the content of Al increases to 3 wt.% and 5 wt.%, the secondary phase changes into $(Mg, Al)_2Ca$ (Fig. 3(c)) and Al_2Ca (Fig. 3(d)), respectively, which distributes continuously along grain boundaries [10]. Some granular secondary phase precipitating at grain interior could also been found in the alloys containing Al elements. The measured volume fractions of precipitates using Image-Pro Plus 5.0 software are 5.7%, 6.7% and 7.2% and 8.3% in AC02, AC22, AC32 and AC52, respectively. This means that the amount of secondary phase increases with the increasing Al content.

Fig. 4(a)–(d) shows the optical micrographs of as-extruded alloys. As compared with the as-cast alloys in Fig. 2, the grains are refined obviously. Alloys containing Al elements have finer grain size than the